International Journal of Nanomedicine

Dovepress

open access to scientific and medical research

Open Access Full Text Article

ORIGINAL RESEARCH

Silica nanoparticles coencapsulating gadolinium oxide and horseradish peroxidase for imaging and therapeutic applications

This article was published in the following Dove Press journal:
International Journal of Nanomedicine
29 November 2012
Number of times this article has been viewed

Nikesh Gupta[1]
Anju Shrivastava[2]
Rakesh K Sharma[1]

[1]Nanotechnology and Drug Delivery Research Lab, Department of Chemistry, [2]Department of Zoology, University of Delhi, Delhi, India

Abstract: Mesoporous silica nanoparticles coencapsulating gadolinium oxide and horseradish peroxidase (HRP) have been synthesized in the aqueous core of sodium *bis*-(2-ethylhexyl) sulfosuccinate (AOT)–hexane–water reverse micelle. The average diameter of these silica particles is around 25 nm and the particles are spherical and highly monodispersed as depicted using transmission electron microscopy. The entrapment efficiency of HRP was found to be as high as 95%. Practically, the entrapped enzyme shows zero leachability up to 90 days. The enzyme entrapped in these silica nanoparticles follows Michaelis–Menten kinetics. Peroxidase entrapped in silica nanoparticles shows higher stability towards temperature and pH change as compared to free enzymes. The gadolinium oxide-doped silica nanoparticles are paramagnetic as observed from the nuclear magnetic resonance line-broadening effect on the proton spectrum of the surrounding water molecule. The entrapped enzyme, HRP, has been used to convert a benign prodrug, indole-3-acetic acid (IAA), to a toxic oxidized product and its toxic effect has been tested on cancerous cell lines through thiazolyl blue tetrazolium blue (MTT) assay. In vitro studies on different cancerous cell lines show that the enzyme has been entrapped and retains its activity inside the silica nanoparticles. IAA alone has no cytotoxic effect and it becomes active only after oxidative decarboxylation by HRP.

Keywords: indole-3-acetic acid, HRP, free radical, cytotoxicity, MRI

Introduction

Enzymes are employed in the body either to replace enzymes that are missing or that are not active in the body. Many enzymes, such as horseradish peroxidase (HRP),[1] glucose oxidase,[2] and other oxidase enzymes,[3] are used for producing the transient free radical species from specific substrates. Recently, it has been reported[4] that the combination of indole-3-acetic acid (IAA) and HRP is cytotoxic to mammalian cells and it was suggested that it could be used as a novel cancer therapeutic approach.[4–7] IAA forms peroxyl-free radical intermediates such as indolyl, skatole, and peroxyl radicals (Scheme 1) after fragmentation of oxidation intermediates.[4,8] Interestingly, neither IAA nor HRP alone show any cytotoxic effect at therapeutic concentrations, but they lead to cell death when used in combination.[9] Free radicals derived from IAA also stimulate the production of reactive oxygen species (ROS), which initiates cellular damage and apoptosis.[10] Therefore, when an enzymatic interaction between HRP and IAA is allowed to take place within the tumor, the IAA is activated and forms free radicals that kill cancer cells by inducing oxidative stress. Excessive accumulation of enzyme molecules to the tumor is often done through antibody-mediated targeting, and the prodrug, IAA, enters the cancer cells from systemic circulation. This therapeutic

Correspondence: Rakesh K Sharma
Department of Chemistry, University of Delhi, Delhi 110007, India
Tel +91 93 1005 0453
Email sharmark101@yahoo.com

Anju Shrivastava
Department of Zoology, University of Delhi, Delhi 110007, India
Tel +91 98 1190 0814
Email ashrivastava@zoology.du.ac.in

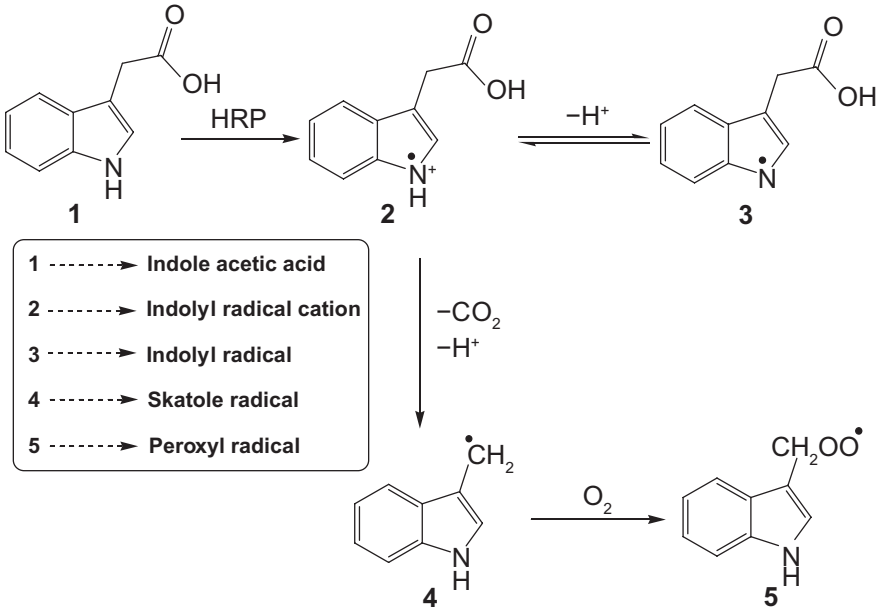

Scheme 1 Diagrammatic representation of oxidation of indole-3-acetic acid by horseradish peroxidase (HRP) to form free radicals.

process is known as antibody-directed enzyme prodrug therapy (ADEPT).[11] Unfortunately, introduction of free enzymes in the body has severe clinical limitations of rapid in vivo degradation by proteolysis and their interactions at multiple receptors.[12] These limitations can be overcome by encapsulating the enzyme in some biocompatible, nonimmunogenic and inert matrix such as silica, which prevents the enzyme from degradation and enzyme substrate reaction can take place by the diffusion of the substrate through the pores. The use of silica nanoparticles (NPs) as the carrier for the enzyme may overcome many limitations, as these are robust, nontoxic, and ultrasmall-sized particles that can easily be eliminated from the body through the kidneys. Silica NPs are useful in many applications, such as biosensors, in vivo tracers, dye-doped nanoparticulate biomarkers, and drug and gene delivery,[13–15] because of their high biocompatibility and low toxicity. Moreover, these particles can be easily prepared with low polydispersity at ambient temperature. Many studies have examined antibody attachment to silica surfaces.[16,17]

Nanoparticle-based molecular imaging has established a unique platform for cellular tracking, targeted diagnostic studies, and image-monitored therapy. The development of NP-based contrast agents for multimodal imaging has attracted considerable interest in biomedical research.[18–21] For these applications, the NPs must have combined properties of high magnetization and functions in the surface area. NPs of lanthanides and their complexes are of current interest due to their strong paramagnetic effects on proton magnetic resonances. Six of the nine elements that display ferromagnetism are lanthanides. The magnetic moments per atom of all six elements are more than that of iron. The gadolinium ion is particularly promising; in fact, it is paramagnetic, with very high magnetic moment per atom[22] and its Curie temperature, 293.2 ± 0.4 K, is close to ambient. Due to the large magnetic moment, these compounds in the forms of their chelating complexes are used as contrast agents for magnetic resonance imaging.[23,24]

We have synthesized silica NPs coencapsulating gadolinium oxide and HRP for imaging as well as enzyme therapeutic purposes. We have demonstrated the HRP-prodrug interaction using silica NPs as host nanocarrier and the consequent impact of the free radicals produced on the human cancer cell lines such as SiHa, a squamous cell carcinoma, MCF-7 breast cancer cells as well as murine cancer cells, and Dalton's T cell lymphoma (DL cells) and, for normal control, murine thymic cells, which are rich in T-lymphocytes. Thus, coencapsulation of inorganic magnetic NPs along with the enzyme has given rise to a completely new dimension for the development of nanomedicine for imaging and therapeutic applications.

Experimental section

Materials

Sodium *bis*-(2-ethylhexyl)sulfosuccinate (AOT; 96%), hexane, gadolinium nitrate pentahydrate, ethanol, and ammonia were purchased from Acrōs Organics (New Jersey, USA), SD Fine Chemicals (Mumbai, India), Central Drug House

(Mumbai, India), Merck (Darmstadt, Germany), and Rankem (Delhi, India), respectively. Tetraethoxysilane (TEOS), dialysis bag (12 kDa), HRP (Rz = 3.0), IAA, and 2,7-dichlorofluorescein diacetate (DCFH-DA) were procured from Sigma Aldrich (St Louis, MO). Millipore water (Millipore, Billerica, MA) was used for preparing solutions and all chemicals were used as such without any further purification.

Synthesis protocol (Scheme 2)

Preparation of HRP-loaded gadolinium oxide nanoparticles

We added 150 µL of Millipore water, 200 µL of gadolinium nitrate ($Gd(NO_3)_3 \cdot 5H_2O$, 0.1 M), and 180 µL of HRP (1.5×10^{-4} M) to 25 mL of 0.1 M AOT in hexane and stirred the solution to give clear microemulsion A. Similarly, clear microemulsion B was prepared by stirring 25 mL of 0.1 M AOT in hexane, containing 150 µL of Millipore water, 200 µL of ammonia (1 M), and 180 µL of HRP of the same concentration. Excess water (100 µL) was added to maintain W_0 (molar ratio of water to AOT in reverse micelle), which in our case is 12.8. Next, microemulsion B was added to microemulsion A drop-wise (11 drops per minute) with constant stirring under cold conditions at 4°C. After completing the addition of B to A, the resultant solution (A + B) was stirred for another 3 hours. Development of slight turbidity indicates the formation of Gd_2O_3 NPs in reverse micelle.

Growth of silica on the surface of HRP-loaded gadolinium oxide NPs

To the above 50-mL reverse micelle containing HRP-loaded gadolinium oxide particles, we added 100 µL of neat TEOS and further stirred the solution for 72 hours at 4°C.

Extraction procedure

To the resultant reverse micelle solution, we added 5 mL of absolute ethanol, which results in the accumulation of silica NPs at the interfacial layer of alcohol and hexane. Next, the particles were separated from the layer by removing the two solutions and washed 3–4 times with an aliquot (5 mL) of ethanol. Finally, the particles were dispersed in 5 mL of Millipore water

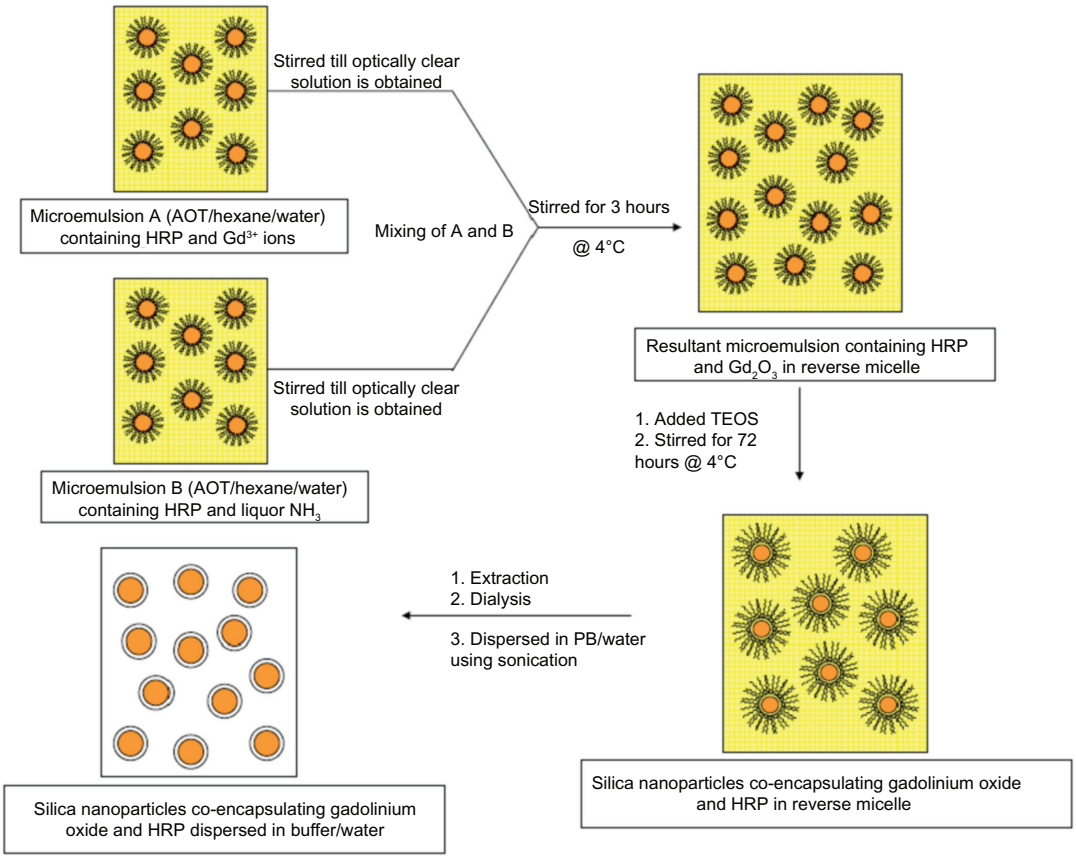

Scheme 2 Diagrammatic representation for the synthesis of silica nanoparticles coencapsulating gadolinium oxide and horseradish peroxidase using water-in-oil microemulsion.

Abbreviations: AOT, sodium *bis*-(2-ethylhexyl)sulfosuccinate; HRP, horseradish peroxidase; PB, phosphate-buffer; TEOS, tetraethoxysilane.

by sonication under cold condition. The dispersed NPs were dialyzed for 12 hours against water using a 12-kDa dialysis membrane bag to remove completely the surfactant and other unreacted and unwanted species. Void NPs were prepared in the same manner, ie, instead of HRP, an equivalent amount of Millipore water was added to maintain the same W_0.

Leachability of the enzyme from the nanoparticles

The leachability of the enzyme from the particles was checked after a regular interval of time. For this, a small volume of the NPs dispersion in buffer was centrifuged at 15,000 rpm for 15 minutes at 4°C so that the particles settled down. Next, the enzyme activity in the supernatant buffer solution was measured spectrophotometrically by treating it with o-dianisidine and H_2O_2 and, from the standard curve, the amount of enzyme was determined.

Characterizations

High-resolution transmission electron microscopy (HRTEM) and energy dispersive spectroscopy (EDS/EDAX)

Measurement was done with a Tecnai G^{2}–30 U-Twin instrument (FEI, Eindhoven, The Netherlands). One drop of the aqueous dispersion of silica NPs coencapsulating Gd_2O_3 and HRP was put on a formvar-coated copper grid and dried under ambient conditions. The dried grid was then examined under an electron microscope.

Dynamic light scattering (DLS)

The measurements were done with a Nicomp™ 380 ZLS instrument (NICOMP Co, Santa Barbara, CA) with an argon-ion air-cooled laser (488 nm) as a light source and recorded at a scattering angle of 90°. The hydrodynamic diameter (*d*) of the NPs was calculated from the diffusion of the particles using the Stoke–Einstein equation.

Proton nuclear magnetic resonance (^{1}H-NMR)

The silica NPs with and without gadolinium oxide-doping were dispersed well in D_2O and a ^{1}H-NMR study was carried out using a 400-MHz spectrometer (JNM-ECX-400P; JEOL, Tokyo, Japan).

Optical studies

All ultraviolet-visible (UV-Vis) spectra were recorded using a Shimadzu-1601 UV-Vis spectrophotometer (Shimadzu, Kyoto, Japan) fitted with a constant temperature cell holder. The temperature of the cell holder was maintained by circulating water around it through a water circulator from Haake Instruments (Pune, India).

Enzyme kinetics

The enzymatic activity of HRP for the catalytic oxidation of o-dianisidine by H_2O_2 was determined spectrophotometrically from the initial slope of the time-dependent absorbance curve of the oxidized product of o-dianisidine having a maximum wavelength (λ_{max}) at 445 nm. Enzyme kinetic studies were performed as follows. Silica NPs coencapsulating Gd_2O_3 and HRP were dispersed in 3 mL of phosphate-buffer (PB; 0.1 M, pH = 7.2). The enzyme kinetics of HRP-catalyzed o-dianisidine oxidation reaction by H_2O_2 was studied by adding 50 µL of o-dianisidine solution (1% w/v) followed by 20–100 µL (20×) of H_2O_2 (1 M) and 20 µL of the NPs dispersed in water/buffer, to 3 mL of 0.1 M PB. The activity of the HRP enzyme is determined from the initial slope of the curve between the increase in absorbance of the colored product measured at 445 nm and the time. The kinetic parameters, K_m and k_{cat}, were calculated from the Lineweaver–Burk plot of the Michaelis–Menten equation in case of free enzyme in aqueous buffer and enzyme coencapsulated with Gd_2O_3 in silica NPs and the values were compared.

Temperature and pH variation

The effect of temperature and pH variation on the activity of free HRP and HRP encapsulated in silica NPs was studied using UV-Vis spectrophotometer. The desired temperature was maintained by circulating water using a water circulator from Haake Instruments. The temperature was varied from 20°C to 70°C and pH was varied from 7.0 to 7.8 at 25°C.

Entrapment efficiency

The entrapment efficiency (*E*%) of HRP in silica NPs was determined from the difference of the total amount of enzyme added in the reverse micelles during preparation and the amount of enzyme remaining unentrapped. The concentration of unentrapped HRP was calculated from a standard curve.

In vitro cytotoxicity through MTT assay

The cytotoxicity of silica NPs with or without encapsulated HRP was compared with free HRP by thiazolyl blue tetrazolium blue (MTT) assay. Two human cancer cells (SiHa, a squamous cell carcinoma, and MCF-7 breast cancer cells, which were maintained according to the instructions provided) and a murine Dalton's lymphoma (DL cells, maintained as ascites by serial transplantation) cells were

seeded at a density of 1.5×10^4 cells/well in a 96-well plate, in 100 µL of RPMI complete media. After 2 hours, cell monolayers were treated with increasing concentrations of IAA (0 to 2 µM) either in the presence of medium alone or in the presence of free HRP (1 µM), void-silica-NPs (SiNPs) or HRP-encapsulated-SiNPs (1 µM). Cells were incubated at 37°C in a humidified environment of 5% CO_2 for 24 hours. Two hours prior to termination of incubation, 20 µL of MTT (5 mg/mL) was added to each well. Two hours postincubation with MTT, the precipitates formed were solubilized by 100-µL isopropanol and quantified by measuring the absorbance at 570 nm (reference wavelength: 620 nm) using a microplate reader (BioTek Instruments, Winooski, VT). We also had control (negative) groups in all MTT assays where we cultured the cells without NP treatments or free HRP or SiNPs-HRP without any cells. All the cancer cells used in the study were obtained from the national cell repository, National Centre for Cell Science (Pune, India). The cells were maintained in culture according to the instructions of the providers.

Free radical determination

Free radicals formed by IAA–HRP combination oxidize DCFH-DA to dichlorofluorescein (DCF). DCFH-DA was activated by taking 350 µL of 1-mM DCFH-DA in ethanol followed by the addition of 1750 µL of 0.01 N NaOH. This mixture was allowed to stand in the dark for 30 minutes followed by the addition of 17.9 mL of 25-mM sodium PB (pH = 7.2). The reaction mixture contains 300 µL of the activated form of DCFH-DA, 40 µL of IAA (500 µM), 40 µL of HRP (1.2 µg/mL), and 3 mL of double-distilled water in a 3.5-mL cuvette. The reaction was studied at room temperature every 10 minutes at λ_{ext} = 490 nm and λ_{em} = 522 nm using a Cary Eclipse fluorescence spectrophotometer (Varian, Palo Alto, CA).

Results and discussion

Silica NPs coencapsulating gadolinium oxide and HRP were prepared in an aqueous core of microemulsion of AOT in hexane. The size of the aqueous core and the particles prepared in the core can be modulated by varying the parameter W_0, which is simply the molar ratio of water to surfactant. We have prepared gadolinium oxide and HRP coencapsulated NPs at W_0 = 12. The strategy involves the polymerization of the silica precursor (TEOS) around the HRP-encapsulated gadolinium oxide NPs in the aqueous core of reverse micelles. The particles obtained using the above protocol are highly monodispersed with spherical morphology. The mean diameter of these particles is around 25 nm as measured using HRTEM (Figure 1A). The average size of these particles comes out to be around 35 nm as measured using DLS (Figure 1B). The small difference in size of these particles measured by the two techniques may be because in TEM we measure the size of the dry powder whereas in DLS we take the size of the particles dispersed in some solvent, which gives us the hydrodynamic diameter of the particles, which is slightly more than the size measured by TEM. The EDAX result (Figure 2) showed the presence of Gd along with the silica. The *E*% of these silica NPs, as measured by the difference of the enzyme added and the enzyme remaining outside, comes out to be around 95% with zero leachability up to 90 days as we observed. The unpaired electron of gadolinium ion in gadolinium oxide is an example of slow electron relaxation, which leads to a line-broadening effect on the protons of the surrounding water molecules (Figure 3B), indicating that the particles could be used for MRI inside the body. In this case, the water protons in the proximity of the gadolinium oxide-doped silica NPs exhibit line broadening with decreased intensity. The water protons, which are not in the proximity of or in the absence of gadolinium oxide, will show the normal (sharp) proton peak

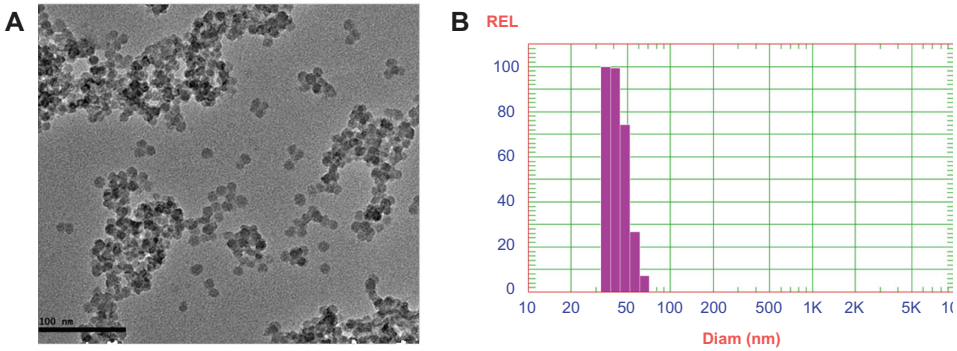

Figure 1 (**A**) Transmission electron microscopic image and (**B**) dynamic light scattering of silica nanoparticles coencapsulating gadolinium oxide and horseradish peroxidase.

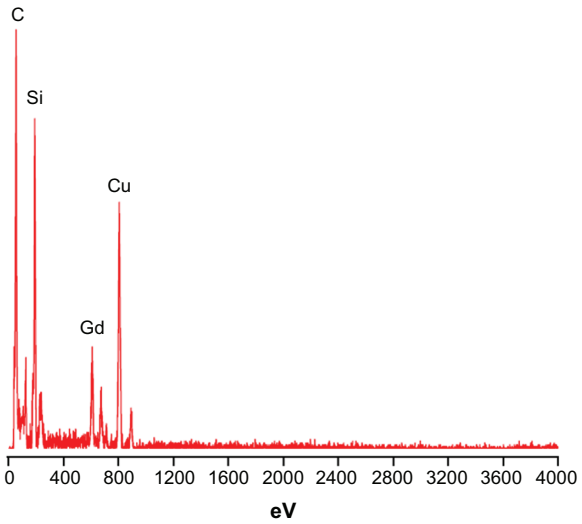

Figure 2 Energy dispersive spectroscopy of silica nanoparticles co-encapsulating gadolinium oxide and horseradish peroxidase indicating the presence of silica and gadolinium.

(Figure 3A). Moreover, the half-line widths in Figure 3A and 3B are different due to the paramagnetic effect of gadolinium on water proton resonance.

The silica NPs entrapping enzyme were dispersed and preserved in PB (0.1 M, pH = 7.2). From the enzyme leachability studies, it was observed that no detectable concentration of HRP was found in the buffer even after 90 days, indicating that the enzyme had not leached out through the pores of the silica matrix. The Michaelis–Menten kinetic parameters[25] k_{cat} and K_m of the free HRP in aqueous buffer and HRP entrapped in silica NPs were calculated from the Lineweaver–Burk plot (Table 1, Figure 4). The lower value of K_m (1.91 mmol/mL) for free HRP in aqueous buffer indicates the high affinity or activity of the enzyme as compared to the HRP entrapped in silica NPs, which have a relatively higher K_m value (16.91 mmol/mL). Since the enzyme is entrapped inside the silica matrix, the substrate has to enter the silica particles through the pores. This imposes some sort of barrier leading to a "diffusional constraint" for the o-dianisidine and H_2O_2 molecule and a subsequent effect on the rate of the enzyme-substrate reaction. The reason for the relatively low activity of the encapsulated HRP may be due to (i) the conformational change of the enzyme in the silica matrices, which caused partial denaturation of the enzyme; (ii) the diffusional constraints of the substrate through the pores of the NPs to reach the enzyme surface entrapped inside; or (iii) both factors simultaneously. The conformational deformation may also result from silylation of the surface hydrophilic groups of the enzymes by TEOS.[26] Depletion in enzymatic activity can also result from the unfavorable orientation of the enzyme active sites for substrate binding inside the silica rigid matrix and a consequent increase in the activation energy for the enzyme substrate reaction. All of these factors, separately or in combination, probably make the activity of the enzyme entrapped in silica NPs lower than the activity of the free enzyme in aqueous buffer. In spite of all these factors, the enzyme entrapped in the silica matrix shows significant activity.

Temperature-dependent activity of the HRP entrapped in silica NPs and free HRP in aqueous buffer (all at pH 7.2) is shown in Figure 5. The activity of the free HRP in aqueous buffer is less at 20°C and increases with increase in temperature until the maximum activity was found to be

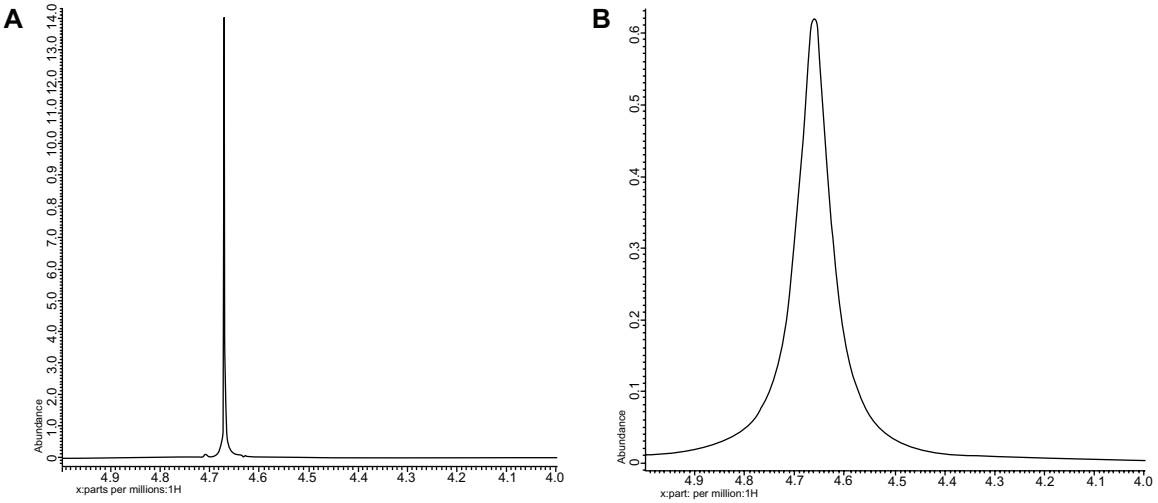

Figure 3 ^{1}H-NMR spectra of the water proton in the vicinity of silica nanoparticles (**A**) without gadolinium oxide and (**B**) with gadolinium oxide.
Abbreviation: ^{1}H-NMR, proton nuclear magnetic resonance.

Table 1 Michaelis–Menten kinetic parameters of free horseradish peroxidase (HRP) and HRP entrapped in silica nanoparticles

Kinetic parameters	Free HRP	Entrapped HRP
K_m (mmol/mL)	1.91	16.91
k_{cat} (min^{-1})	5.1×10^4	4.2×10^3

at 38°C as reported previously.[27] After the maximum, the activity starts decreasing with further rise in temperature. Similar behavior was obtained in the case of the entrapped HRP except that the maximum activity was found at 60°C. (Activity measurements beyond 70°C are not reliable results due to the formation of bubbles in the cuvette.) This shows that, although the entrapped enzyme is less active than the free enzyme, it is also less sensitive to temperature change than the free enzyme. The temperature profile for the activity of the entrapped enzymes is quite broad. This is perhaps because the heat-resistant silica matrix protects the entrapped enzyme and restricts its mobility from temperature-induced denaturation, thereby increasing its stability over a wider range of temperatures.

Figure 6 shows the dependence of HRP activity on the pH of the buffer solution in the entire pH range from 7 to 7.8. The free enzyme shows maximum activity at pH = 7.2, whereas the entrapped enzyme in silica NPs does not show any maximum, up to pH = 7.8. (Above this pH, no measurement was performed because of auto-oxidation of the substrate in alkaline medium.) This is a typical trend expected for an enzyme entrapped in a negatively charged matrix such as silica.[28] The polyionic matrices of charged silica particles should have the general effect of causing a partitioning of protons between the bulk phase and the enzyme microenvironment. Such proton partitioning in the encapsulated enzymes system and the consequent shift of pH maximum are also observed in the case of charged polymeric NPs.[29] The pH profile curve of the entrapped enzyme is broader than that of the free enzyme. This shows that the entrapped enzyme is more resistant to pH-dependent activity changes than the free enzyme as a result of being entrapped inside the rigid silica matrix, which acts as a "protective shell" for the entrapped enzyme.

The IAA–HRP combination leads to the formation of indolyl, skatole, and peroxyl radicals, hence we measured the production of these radicals using DCFH-DA. From Figure 7, it can be concluded that DCFH-DA is being oxidized to DCF, and the formation of DCF from DCFH-DA depends purely upon free radicals such as indolyl, skatole, and peroxyl. Therefore, it can be stated that the IAA–HRP combination

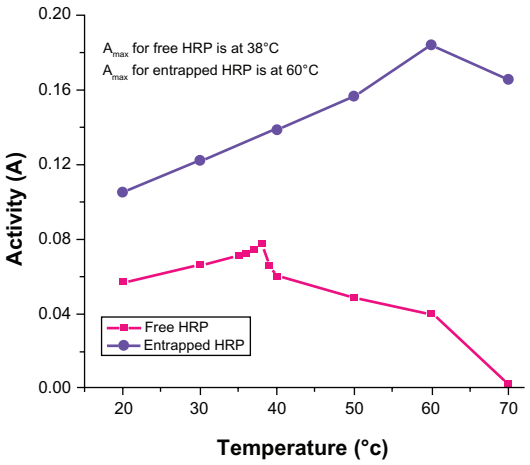

Figure 5 Temperature-dependent enzymatic activity of horseradish peroxidase (HRP; free and entrapped) during oxidation of o-dianisidine by H_2O_2 in phosphate-buffer (pH = 7.2) measured in the range of 20°C–70°C.

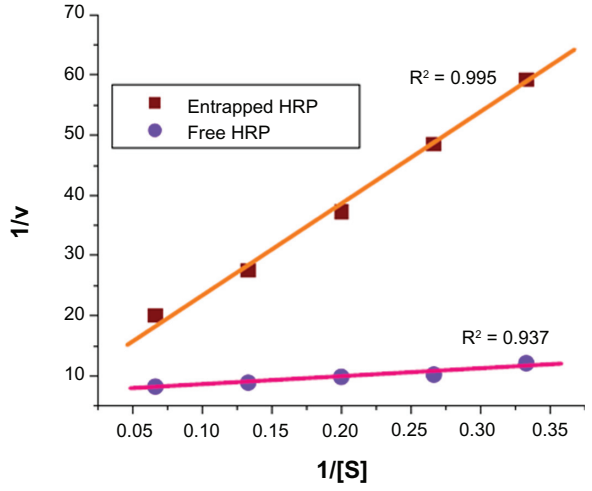

Figure 4 Lineweaver–Burk plot for comparison of Michaelis–Menten parameters of free horseradish peroxidase (HRP) and HRP entrapped in silica nanoparticles.

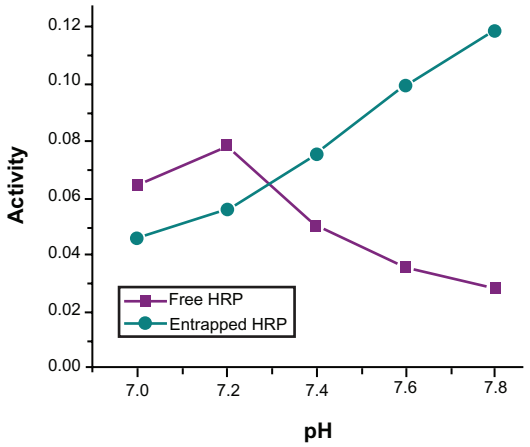

Figure 6 pH-dependent catalytic activity of horseradish peroxidase (HRP; free and entrapped) during oxidation of o-dianisidine by H_2O_2 in phosphate-buffer (pH = 7.2) at 25°C.

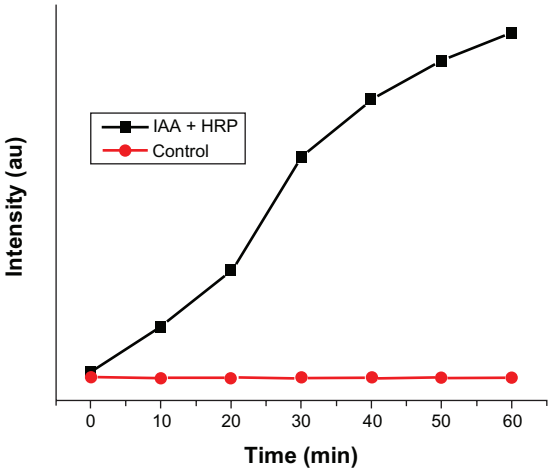

Figure 7 Kinetic study for the formation of DCF from DCFH-DA due to IAA–HRP combination.
Abbreviations: DCF, dichlorofluorescein; DCFH-DA, 2,7-dichlorofluorescein diacetate; HRP, horseradish peroxidase; IAA, indole-3-acetic acid.

leads to the formation of free radicals, which are responsible for the killing of cancer cells.

In order to determine the possibility of using these HRP entrapped silica NPs for converting a benign prodrug, IAA, into a cytotoxin, we performed an in vitro cytotoxicity assay. For this assay, we used human cancer cell lines such as SiHa, MCF-7, DL cells and normal murine thymic cells. These cells were incubated with increasing concentration of IAA (0 to 2 μM) in either medium alone or in combination with free HRP, void SiNPs, or SiNPs-entrapped HRP. Cell viability was measured using the MTT assay after 24 hours of treatment. From the results (shown in Figure 8), we observed significant cell death in all of the three cancer cells incubated with the free IAA–HRP combination. On the other hand, no significant difference in cell death was observed in the normal thymic cells with or without the IAA–HRP combination. Further,

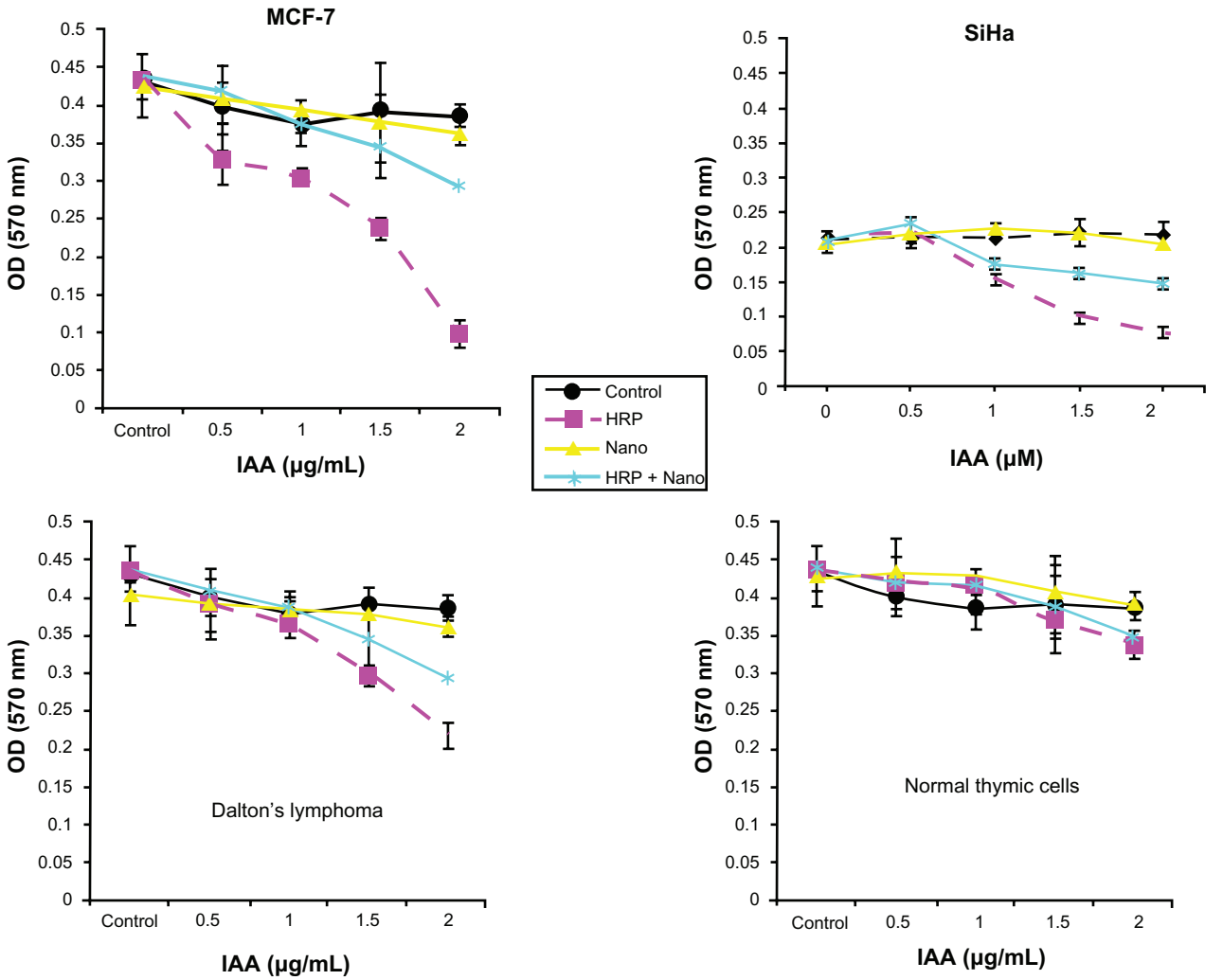

Figure 8 Cytotoxicity studies (MTT assay) of void silica nanoparticles (Nano), free HRP and HRP entrapped in silica nanoparticles (HRP + Nano) on SiHa, MCF-7, Dalton's lymphoma, and normal thymic cell lines.
Abbreviations: IAA, indole-3-acetic acid; MTT, thiazolyl blue tetrazolium blue; HRP, horse radish peroxidase.

when cells were treated with a SiNPs-entrapped HRP-IAA combination, SiHa and DL cells were found to be more sensitive compared to MCF-7 cells. Within 24 hours, about 50% of SiHa and DL cells died at 2-μM IAA with SiNPs-entrapped HRP combination treatment, whereas, relatively fewer cell deaths (30%–35%) were induced in MCF-7 cells with the same treatment. It took at least 72 hours to induce significant cell death in MCF-7 cells with the SiNPs entrapped HRP-IAA combination (data not shown). These differences between different cell lines are not surprising. The observed difference between MCF-7 and SiHa or DL cells could be, among others, caused by different uptake rates, and this needs to be confirmed. The rates of proliferation of the cell lines were different. As compared to MCF-7, SiHa and DL cells were relatively fast proliferating, which may also contribute to differences in uptake and hence sensitivity. Neither IAA alone nor its combination with void SiNPs resulted in any cell killing. The results thus show that the IAA–HRP combination can kill the tumor cells. Entrapment did not show any significant reduction in activity of the enzyme. Also, entrapped HRP can be active for a relatively longer duration and at wider pH range. Additionally, in order to rule out any influence of HRP in formazan bioreduction in MTT assay, we incubated the free HRP or SiNPs-HRP without cells for 24 hours and added MTT to this solution in a similar manner as to the treated cells. We did not observe any significant difference in OD from the blank wells where the MTT was added to the medium alone without any cells, suggesting that the formazan bioreduction observed in cells with and without IAA–HRP treatment were due to the presence of live cells. Since tumor cells usually possess higher levels of scavengers for ROS, they may be more vulnerable to the combination of silica NPs entrapped HRP and IAA. Thus, it would be useful to develop strategies for effective use of encapsulated HRP in cancer treatment.

Conclusion

Gadolinium oxide and HRP can be coencapsulated in the core of silica NPs by utilizing the aqueous core of water-in-oil microemulsion as host nanoreactor. The particle size can be modulated by varying the parameter W_0, which is the water-to-surfactant ratio. When prepared at a W_0 of 12, the particles are around 25 nm in diameter with spherical morphology and are reasonably monodispersed. The enzyme entrapment efficiency of the silica NPs comes out to be more than 95% with zero leachability of the enzyme up to 90 days as we observed. The entrapped gadolinium ion causes a line broadening of water proton which is present in the proximity of Gd_2O_3 whereas silica nanoparticles without Gd_2O_3 shows no such peak broadening in ^{1}H-NMR spectra, indicating that the particles could be used for MRI. The kinetic parameters of the entrapped enzyme were determined and compared with that of free enzymes. The catalytic activity of the entrapped enzyme is less than that of free enzymes, which may be due to the diffusional constraint of the substrate. Although the activity of the entrapped enzyme is less, it is still sufficient to be used for enzyme therapeutic purpose. The MTT assay with these particles shows that neither IAA alone nor its combination with void SiNPs resulted in any tumor cell killing whereas the IAA–HRP combination can kill the cells. Entrapment did not show any significant reduction in activity of the enzyme. Also, entrapped HRP can be active for a relatively longer duration. Thus, coencapsulation of gadolinium oxide along with the enzyme gives a completely new dimension for the development of new diagnostic and therapeutic agents.

Acknowledgments

NG and RKS are grateful for financial assistance from the University Grants Commission, Government of India, and the University of Delhi. NG is grateful for the award of a Senior Research Fellowship by the Council of Scientific and Industrial Research (CSIR, Delhi). AS is grateful for a DU-DST Purse grant from the University of Delhi and DST. The authors are grateful for the valuable comments and fruitful discussion with Prof Amarnath Maitra and Dr Indrajit Roy, Department of Chemistry, University of Delhi.

Disclosure

The authors report no conflicts of interest in this work.

References

1. Kim DS, Jeon SE, Jeong YM, Kim SY, Kwon SB, Park KC. Hydrogen peroxide is a mediator of indole-3-acetic acid/horseradish peroxidase-induced apoptosis. *FEBS Lett*. 2006;580:1439–1446.
2. Trivic S, Leskovac V, Zeremski J, Vivic M, Winston GW. Bioorganic mechanisms of formation of free radicals catalyzed by Glucose oxidase. *Bioorg. Chem*. 2002;30:95–106.
3. Cheeseman KH, Slater TF. An introduction of free radical biochemistry. *Br Med Bull*. 1993;49:481–493.
4. Folkes LK, Candeias LP, Wardman P. Toward targeted "oxidation therapy" of cancer: peroxidase-catalysed cytotoxicity of indole-3-acetic acids. *Int J Radiat Oncol Biol Phys*. 1998;42:917–920.
5. Manda G, Nechifor MT, Neagu TM. Reactive oxygen species, cancer and anti-cancer therapies. *Curr Chem Biol*. 2009;3:342–366.
6. Trachootham D, Alexandre J, Huang P. Targeting cancer cells by ROS-mediated mechanisms: a radical therapeutic approach. *Nat Rev Drug Discov*. 2009;8:579–591.
7. Huh SY, Na JI, Huh CH, Park KC. The effect of photodynamic therapy using indole-3-acetic acid and green light on acne vulgaris. *Curr Pharm Des*. 2002;8:1363–1374.

8. Candeias LP, Folkes LK, Porssa M, Parrick J, Wardman P. Enhancement of lipid peroxidation by indole-3-acetic acid and derivatives: substituent effects. *Free Radic Res*. 1995;23:403–418.
9. Pugine S, Piza T, Costa E, De Melo M. Toxicity of indole-3-acetic acid combined with horseradish peroxidase on Staphylococcus aureus. *Webmed Central Microbiology*. 2010;1:WMCOO695.
10. Kim DS, Jeon SE, Park KC. Oxidation of indole-3-acetic acid by horseradish peroxidase induces apoptosis in G361 human melanoma cells. *Cell Signal*. 2004;16:81–88.
11. Andrady C, Sharma SK, Chester KA. Antibody-enzyme fusion proteins for cancer therapy. *Immunotherapy*. 2011;3:193–211.
12. Pernot M, Vanderesse R, Frochot C, Guillemin F, Barberi-Heyob M. Stability of peptides and therapeutic success in cancer. *Expert Opin Drug Metab Toxicol*. 2011;7:793–802.
13. Bhakta G, Sharma RK, Gupta N, Cool S, Nurcombe V, Maitra A. Multifunctional silica nanoparticles with potentials of imaging and gene delivery. *Nanomedicine*. 2011;7:472–479.
14. Bharali DJ, Klejbor I, Stachowiak EK, et al. Organically modified silica nanoparticles – a novel non-viral vector for in vivo gene delivery and expression in the brain. *Proc Natl Acad Sci U S A*. 2005;102:11539–11544.
15. Santra S, Yang H, Dutta D, et al. TAT conjugated, FITC doped silica nanoparticles for bioimaging applications. *Chem Commun*. 2004;24:2810–2811.
16. Bagshawe KD, Sharma SK, Begent RH. Antibody-directed enzyme prodrug therapy (ADEPT) for cancer. *Expert Opin Biol Ther*. 2004;4:1777–1789.
17. Niculescu-Duvaz I, Springer C. Antibody-directed enzyme prodrug therapy (ADEPT): A review. *Adv Drug Deliv Rev*. 1997;26:151–172.
18. Selvan ST, Tan TTY, Yi DK, Jana NR. Functional and multifunctional nanoparticles for bioimaging and biosensing. *Langmuir*. 2010;26:11631–11641.
19. Cheon J, Lee JH. Synergistically integrated nanoparticles as multimodal probes for nanobiotechnology. *Acc Chem Res*. 2008;41:1630–1640.
20. Kim J, Piao Y, Hyeon T. Multifunctional nanostructured materials for multimodal imaging, and simultaneous imaging and therapy. *Chem Soc Rev*. 2009;38:372–390.
21. Wang F, Liu X. Recent advances in the chemistry of lanthanide-doped upconversion nanocrystals. *Chem Soc Rev*. 2009;38:976–989.
22. Voisin P, Ribot EJ, Miraux S, et al. Use of lanthanide grafted inorganic nanoparticles as effective contrast agent for cellular uptake imaging. *Bioconjug Chem*. 2007;18:1053–1063.
23. Bohigas X, Molins E, Roig A, Tegada J, Zhang XX. Magnetic moments of gadolinium ions. *IEEE Trans Magn*. 2000;36:538–544.
24. Morawski AM, Lanza GA, Wickline SA. Targeted contrast agents for magnetic resonance imaging and ultrasound. *Curr Opin Biotechnol*. 2005;16:89–92.
25. Wikipedia. Michaelis–Menten kinetics. August 8, 2012. Available from: http://en.wikipedia.org/wiki/Michaelis-Menten_kinetics. Accessed on August 10, 2012.
26. Ahn HS, Shin HS. Determination of ethylene oxide-hemoglobin adduct by silylation and gas chromatography-electron impact-mass spectrometry. *J Chromatography B*. 2006;843:202–208.
27. Sharma RK, Das S, Maitra A. Enzymes in the cavity of hollow silica nanoparticles. *J Colloid Interf Sci*. 2005;284:358–361.
28. Wang W, Gu B, Liang LJ. Effect of anionic surfactants on synthesis and self-assembly of silica colloidal nanoparticles. *J Colloid Interf Sci*. 2007;313:169–173.
29. Trevan MD. Chapter 2. In: *Immobilized Enzymes: An introduction and applications in biotechnology*. New York, NY: John Wiley & Sons; 1980.